School of Mechanical, Aerospace & Automotive Engineering

Faculty of Engineering, Environment and Computing

Coventry, United Kingdom

6063MAA Coursework 1

Written By:

Ravi Chaudhary, 10947986

Agris Gavars, 10308903

Emils Pless, 10326491

Jenner Romero Leon, 9699487

Table of contents

List of figures

List of tables

Abstract

This report covers the development and validation of a 2D CFD model of a concentric tube heat exchanger. An experiment was preformed, where the effectiveness and other parameters of a TD360a heat exchanger was calculated based on changing heater temperatures and changing flow rates in parallel flow configuration. A 2D model was developed and simulations were performed with the same inputs as the experiment. The details of the creation of a 2D simulation were explained alongside with the sources of errors and applicability. The results of both methods were evaluated and compared.

Introduction and theory

Background

Heat exchangers are systems that exchange heat between fluids or gasses. The fluids or gasses are not allowed to mix with each other. The heat transfer is facilitated through a thin wall separating the two elements. Some applications of heat exchangers are domestic and industrial radiators, refrigerators, power generation systems and many more (Team, 2021).

There are different ways to classify heat exchangers. The flow of the two fluids or gasses can be arranged in parallel flow, counter flow, and cross flow configuration. All flow arrangements have their own applications as the efficiency of each flow configuration depends on specific conditions of each heat exchanger unit. The difference between counter flow and parallel flow is very noticeable when plotting the temperature (*Figure 1*). A large temperature difference at the ends in immediately noticeable, this can cause thermal stress on the heat exchange (Edge., 2019). Parallel configuration is advantageous if the aim is to bring the temperatures close together, however counter flow configuration makes for a steadier heat transfer rate as the temperature difference does not change as much. It is important to note that the main parameter driving the heat exchange is the temperature difference, which imposes some limitations, such as the minimum or maximum temperature the fluids can achieve. Cross flow configuration is more often used in combination with air, such as a car radiator, as a large area is usually required to achieve effective heat exchange.

Figure 1: Parallel and Counter flow

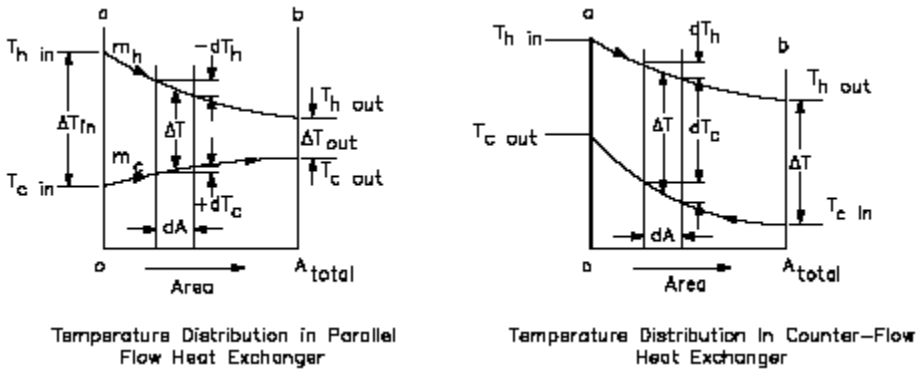

Note. (Engineers Edge, 2022).

Other ways to classify heat exchangers are based on whether the flow is mixed or unmixed. Unmixed flow is channelled through the heat exchanger by fins to prevent mixing within the fluid or gas, mixed fluid on the other hand is flowing freely and mixing continuously (figure 2.). Mixed and unmixed flow effects the heat transfer rate due to the behaviour of the flow and the pressure changes.

Figure 2: Mixed and Unmixed flow

Note. (Linquip, 2021).

Heat exchangers have different designs, such as shell and tube, double pipe, plate heat exchangers and more. Different designs change how the fluid or gas is passing through the heat exchanger, affect the applications and limitations of heat exchangers, as well as manufacturing costs and maintenance. Figure 3 depicts the different configurations of inner tubes, which greatly affects the rate of heat exchange and can reduce the size of the heat exchanger.

Figure 3: Tubular pipe configuration of inner tubes

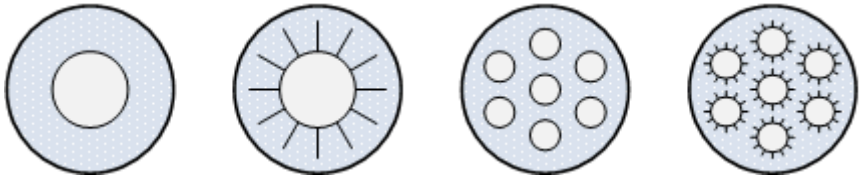

Note. (Alternative Energy Tutorials, n.d.).

Multiple pass heat exchangers refer to how many times the inner tube and shell passes (figure 4.). The main application of multiple pass configurations is found in thermal power generation and refrigeration systems.

Figure 4: Multiple pass heat exchanger

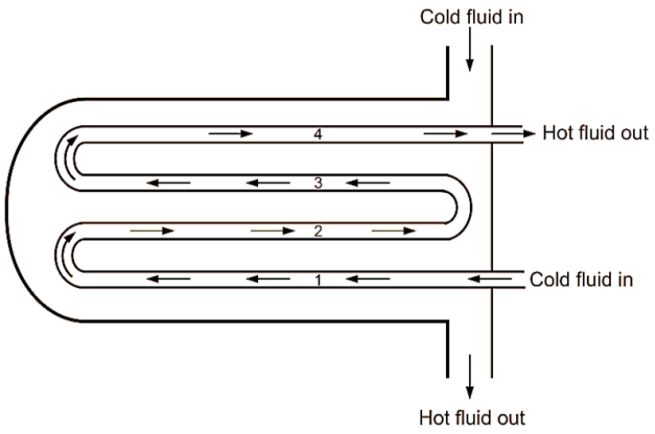

Note. (Electrical Workbook, 2022).

Problem description

In recent years CFD simulations have become the main way to solve complicated fluid and thermodynamics problems. All CFD models are simulations, thus can sometimes produce unreliable results depending on the complexity of the simulation and parameters included (De Luca et al., 2016). The validation of CFD models has become an important aspect of developing practical and accurate solutions to real life problems.

This experiment uses a concentric tube TD360a heat exchanger in counter flow configuration as shown in figures 5 and 6. The inner tube is made from steel and carries the hot water, whereas the acrylic shell encompasses the cold water. The temperature is measured at the beginning and end for both hot and cold flow.

Figure 5: Counter flow configuration

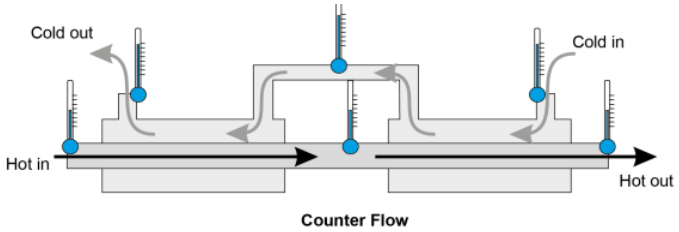

Note. Figure taken from CW1 brief (Qubeissi, 2022).

Image 1: TD360a concentric pipe heat exchanger

Note. Own creation.

Design modeller

Ansys 2019 was used to develop a 2D design of heat exchanger. The specifications of a TD360a heat exchanger were considered to create a 2D geometry which is tabulated in table 1. The front view of the 2D model is shown in Figure 6.

Figure 6: Front View of 2D Geometry with labels

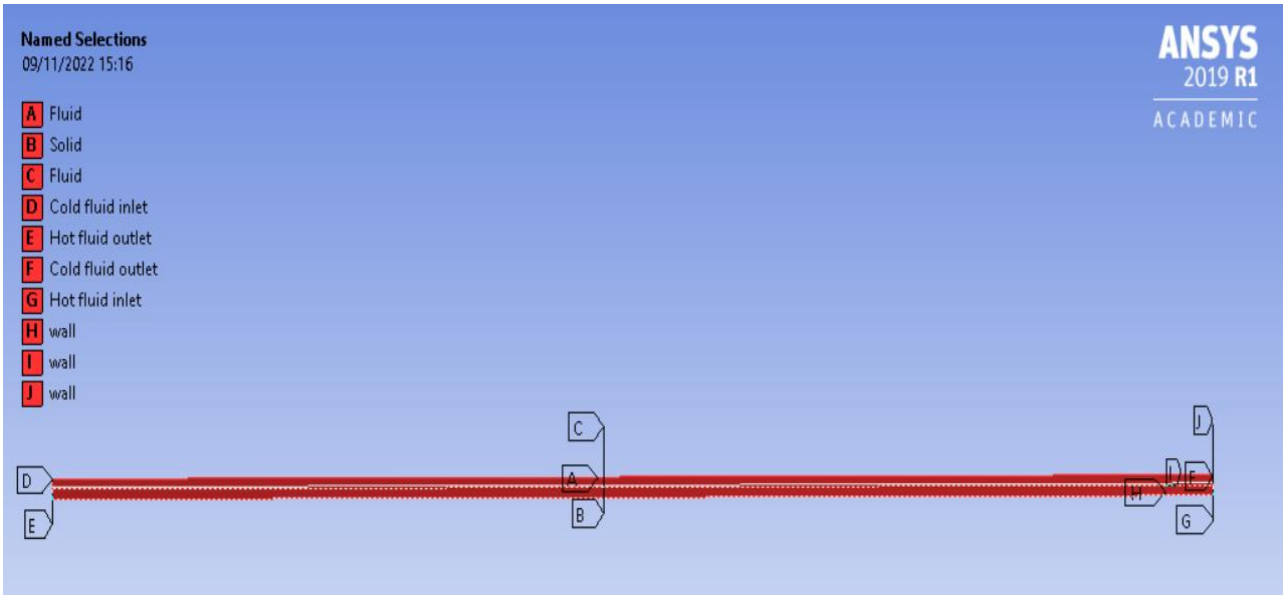

Note. Own creation.

Table 1: TD360a dimensions

	Inner tube (mm)	Outer tube (mm)
Length of tube	700	700
Tube diameter	10	20
Thickness	1	5

Note. Own creation.

Meshing techniques

The crated mesh is shown in figure 7. Utilizing different meshes in order to achieve the best outcomes is crucial. To enhance mesh quality of the 2D model of heat exchanger, techniques like the automatic method, face meshing, and refinement were applied. To enhance the outcomes, factors such as element quality, skewness, and orthogonal quality (figure 8) were prioritized. For this specific model, the best mesh that was achieved consists of 54201 nodes and 52304 elements with a 1.5mm element size. An average orthogonal quality of 1 and an average skewness quality of 1.53*10^ (-10) were obtained by using the meshing technique specified above. A high-quality mesh helps to get more accurate results, whereas a low-quality mesh causes convergence issues. The result of that leads to inaccurate results and false conclusions. Cells in the 2D mesh are triangular and quadrilateral in shape and the ideal cell shape for this 2D geometry was found to be quadrilateral. The mesh will be more likely to have fewer cells if triangular cells are used, but the mesh quality will be marginally worse. Due to which, it might cause a negative impact on the accuracy, desired skewness, and orthogonal quality of convergence. Additionally, mesh refinement was used as an editing tool to improve solution accuracy.

Figure 7: Created mesh with an element Size of 1.5 mm

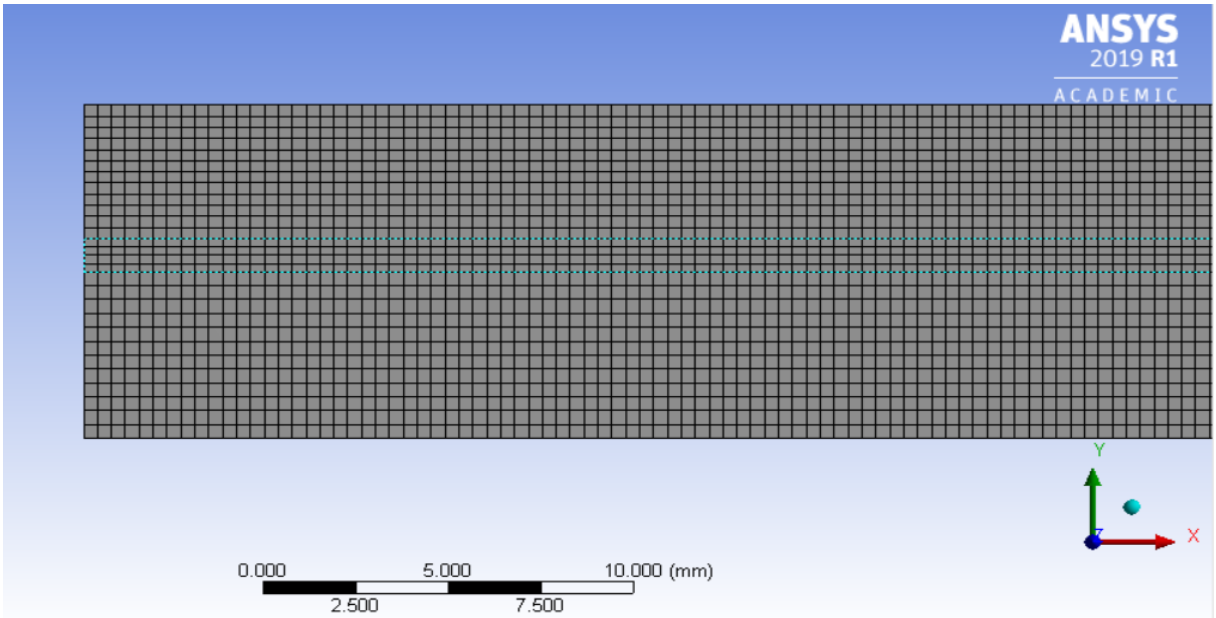

Note. Own creation.

Figure 8: Skewness and orthogonal quality mesh metrics spectrums

Skewness mesh metrics spectrum

Excellent	Very good	Good	Acceptable	Bad	Unacceptable
0-0.25	0.25-0.50	0.50-0.80	0.80-0.94	0.95-0.97	0.98-1.00

Orthogonal Quality mesh metrics spectrum

Unacceptable	Bad	Acceptable	Good	Very good	Excellent
0-0.001	0.001-0.14	0.15-0.20	0.20-0.69	0.70-0.95	0.95-1.00

Note. (Tips., 2021).

Model geometry

The heat exchanger was drawn along the x-axis and due to the limitation of the 2D solver in reference to solving the Navier Stokes equation in only X and Y axis, the one side of the pipe was sketched, and another size of the pipe was added within it which increased the length of the pipe. Similarly, due to its symmetricity, the pipe was rotationally cut, and the axis was defined in order to minimise the amount of computing power needed to simulate the flow.

Setup conditions

- The energy equation was turned on, and the viscous model was set to be k-epsilon, realizable and enhanced wall treatment. The k-epsilon model was set due to the transient flow which was determined after calculating the Reynold's number.

- Both the outer and inner pipe were set to be the solids and the outer pipe material properties were added as of acrylic (PMMA). Similarly, the stainless steel was selected for the inner pipe material.
- Fluids in the inner pipe as well as the fluid in the outer pipe were specified as water-liquid (H2O).
- In the cell zone condition, the cold-water fluid domain and the hot water fluid domain were set to cold-water liquid and hot-water liquid, respectively. Either way the properties of both the cold and hot water were almost similar.
- The boundary condition setup for this model were listed as:

  Cold Inlet temperature- 21.4 degree Celsius

  Hot inlet temperature- 51.4 degree Celsius

  Velocity inlet (Cold flow): 0.395 m3/s

  Velocity inlet (Hot flow): 0.151 m3/s

  The above boundary condition was for one of the temperature experiments carried out during the lab and was changed according to different experiments.

  The thickness of inner pipe was created as 1mm rather than specifying separately in the geometry.
- The convergence absolute criteria in the residual section of monitor were set to 1*10^ (-6).
- The surface integrals of hot inlet, hot outlet, cold inlet, and cold outlet were considered.
- The initialization was done, and the simulation was run till the residuals converges.

Assumptions

- Steady and fully developed flow.
- Constant hot and cold temperatures.
- No heat loss.
- No backflow.

Mesh Independence Check

The mesh independence was checked applying the coarse mesh with bigger element size to the finer mesh with the smaller element size. The mesh quality was constantly improved using various meshing techniques such as automatic method, face meshing, and refinement. The mesh independence results were tabulated in table 2.

Table 2: Mesh independence of 2D model

Element size (m)	Number of elements	Hot outlet temperature (Celsius)	Cold outlet temperature (Celsius)
30*10^(-3)	**1344**	**47.12666**	**23.514102**
10*10^(-3)	**4480**	**46.223928**	**24.211393**
6.0381*10^(-3)	**5568**	**46.209376**	**24.70002**
3*10^(-3)	**14912**	**45.891689**	**24.201755**
2*10^(-3)	**33600**	**45.891098**	**24.223763**
1.5*10^(-3)	**52304**	**45.78233**	**24.259822**

Note. Own creation.

The following figures 9 and 10 show the outlet temperature results depending on the number of elements.

Figure 9: Hot outlet temperature vs number of element generated during mesh independence study

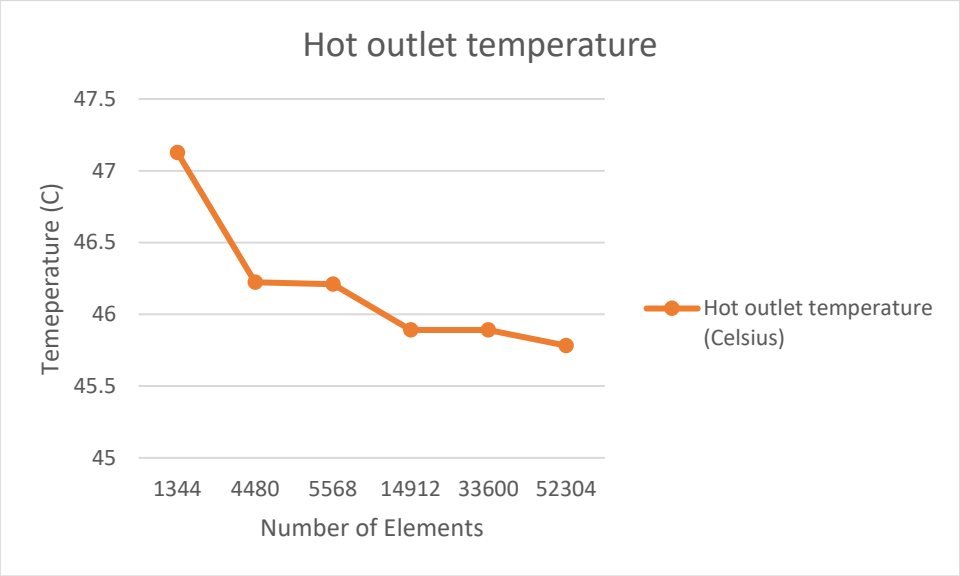

Note. Own creation.

Figure 10: Cold outlet temperature vs number of element generated during mesh independence study

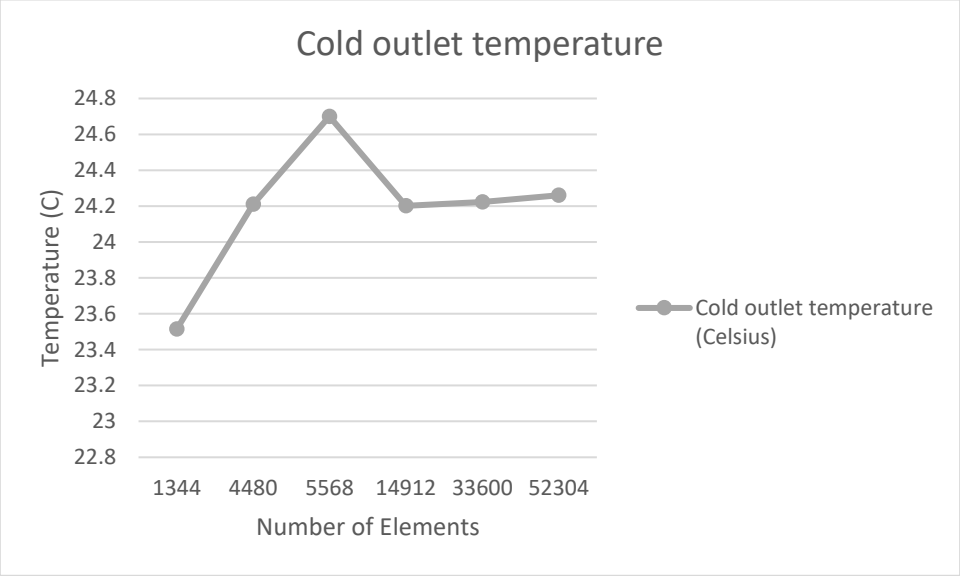

Note. Own creation.

Figures 9 and 10, show a decrease in the hot outlet temperature and an increase in the cold outlet temperature with a decreasing element size. If the mesh is of good quality, the temperature generally approaches the experimental values. The mesh used for the 30*10(-3) element was of poor quality, resulting in a different temperature from that of the better mesh.

Test and analysis

Theoretical calculations

After the experiment was performed the data was compiled and the following calculations were performed.

- Mean hot temperature: $\overline{T_H} = \frac{\mathrm{Th1} + \mathrm{Th2}}{2} = \frac{51.1 + 42.9}{2} = 8.2$ °C
- Mean cold temperature: $\overline{T_C} = \frac{\mathrm{Tc1} + \mathrm{Tc2}}{2} = \frac{20.9 + 24.7}{2} = 3.8$ °C
- Efficiency for hot flow: $\eta_h = \frac{T_{h1} - T_{h2}}{T_{h1} - T_{c1}} = \frac{51.1 - 42.9}{51.1 - 20.9} = 27.15$ %
- Efficiency for cold flow: $\eta_c = \frac{T_{c2} - T_{c1}}{T_{h1} - T_{c1}} = \frac{24.7 - 20.9}{51.1 - 20.9} = 12.58$ %
- Mean temperature efficiency: $\bar{\eta} = \frac{\eta_h + \eta_c}{2} = \frac{27.15 + 12.58}{2} = 19.87$ %
- Power emitted: $\dot{Q}e = V_h * \rho_h * C_{ph} * \Delta T_h$ = 0.000011 * 989.44 * 4179.56 * 8.2 = 373.02 W
- Power absorbed: $\dot{Q}a = V_c * \rho_c * C_{pc} * \Delta T_c$ = 0.000027 * 997.61 * 4180.18 * 3.8 = 425.22 W
- Energy balance coefficient: $C_{EB} = \frac{\dot{Q}a}{\dot{Q}e} = \frac{425.22}{373.02} = 1.14$
- Logarithmic mean temperature difference: LMTD = $\frac{(T_{h1} - T_{c2}) - (T_{h2} - T_{c1})}{\ln(\frac{(T_{h1} - T_{c2})}{(T_{h2} - T_{c1})})}$ =

  $= \frac{(51.1 - 24.7) - (42.9 - 20.9)}{\ln(\frac{(51.1 - 24.7)}{(42.9 - 20.9)})} = 24.13$ °C

- Heat transfer coefficient: $U = \frac{\dot{Q}_e}{A * LMTD} = \frac{373.02}{0.02 * 24.13} = 772.94$ W/m^2 * K

Results

Experimental results

For experiment 1 the heater temperatures and hot flow rates were kept constant. The aim of this experiment was to show the effect of varying cold flow rates on the performance of the heat exchanger. The results of experiment 1 were shown in table 3.

For experiment 2 both cold and hot water flow rates were fixed at 1.59 L/min. The aim of experiment 2 was to show the effect of different hot water supply temperatures on the heat exchanger. The results of experiment 2 are shown in table 4.

Both experiments were performed in counter flow configuration.

Table 3: Experiment 1 results

Hot flow, L/min	Cold flow, L/min	Th1, °C	Th2, °C	Δ Th, °C	$\overline{T_h}$, °C	Tc1, °C	Tc2, °C	Δ Tc, °C	$\overline{T_C}$, °C	$\eta_{h,\%}$	$\eta_{c,\%}$	ρ_h, kg/m^3	ρ_c, kg/m^3	C_{ph}, J/(kg K)	C_{pc}, J/(kg K)	Q_e, W	Q_a, W	C_{EB}	$\bar{\eta}$, %	LMTD, °C	U, W
0.66	1.61	51.1	42.9	8.2	46.8	20.9	24.7	3.8	22.7	27.15%	12.58%	989.44	997.61	4179.56	4180.18	373.02	425.22	1.14	19.87%	24.13	772.9
0.73	1.41	51.6	43.3	8.3	47.5	20.1	23.6	3.5	21.9	26.35%	11.11%	989.14	997.47	4179.73	4180.54	417.50	342.98	0.82	18.73%	25.53	817.7
0.73	1.19	51.4	43.7	7.7	47.4	21.6	25.9	4.3	28.9	25.84%	14.43%	989.18	997.37	5179.71	4179.76	480.00	355.53	0.74	20.13%	23.76	1010.1

Note. Own creation.

Table 4: Experiment 2 results

Hot flow, L/min	Heater temperature, °C	Th1, °C	Th2, °C	Δ Th, °C	$\overline{T_h}$, °C	Tc1, °C	Tc2, °C	Δ Tc, °C	$\overline{T_C}$, °C	$\eta_{h,\%}$	$\eta_{c,\%}$	ρ_h, kg/m^3	ρ_c, kg/m^3	C_{ph}, J/(kg K)	C_{pc}, J/(kg K)	Q_e, W	Q_a, W	C_{EB}	$\bar{\eta}$, %	LMTD, °C	U, W
0.71	55.6	51.0	44.5	6.5	47.6	20.8	24.2	3.4	22.5	21.52%	11.26%	989.10	997.65	4179.76	4180.26	318.00	281.20	0.88	16.39%	25.22	630.4
0.8	50.2	50.0	43.9	6.1	46.9	19.4	22.7	3.3	30.3	19.93%	10.78%	989.40	997.97	4179.58	4180.95	336.34	364.88	1.08	15.36%	25.88	649.8
0.78	48.1	48.2	42.2	6.0	45.0	19.1	22.2	3.1	20.7	20.62%	10.65%	990.21	998.06	4179.15	4181.17	322.78	342.82	1.06	15.64%	24.52	658.2

Note. Own creation.

Figures 11 and 12 plot the temperatures of cold and hot flow within the heat exchanger. The graphs produced are consistent with what is expected from counter flow configuration. It is important to note that the hot flow in red is moving to the right of the graph whereas the cold flow in blue is moving to the left of the graph. An example for flow directions can be found in figure 1 on page 2.

Figure 11: Experiment 1 results graph

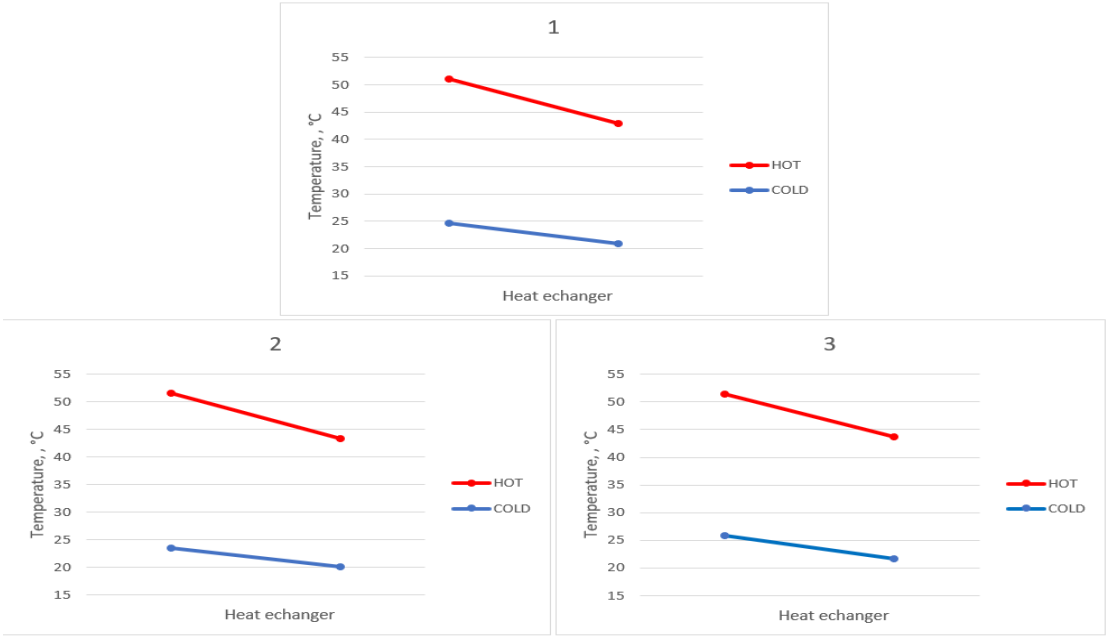

Note. Own creation.

Figure 12: Experiment 2 results graph

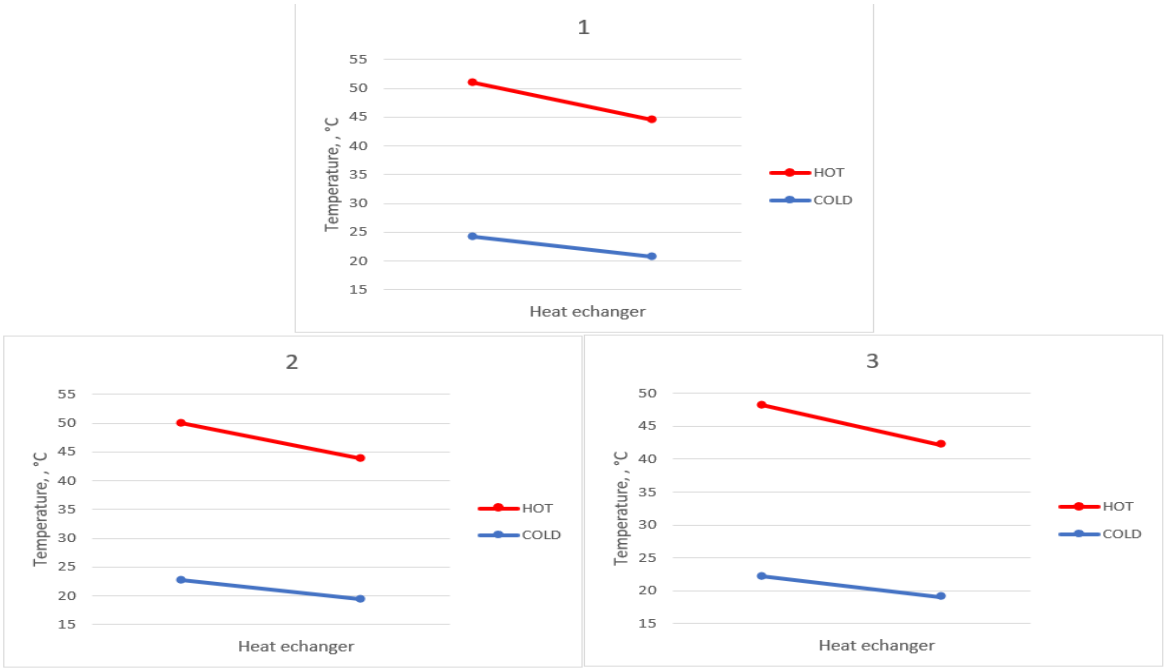

Note. Own creation.

CFD results

The 2D model was successfully run and the produced results were compiled in this section using figures and tables. The 2D model was not very hardware intensive and took around 3 to 4 minutes to run.

As shown in figure 13 nearly all the residuals have been reduced to 6 orders of magnitude or less and have met the convergence criteria of 1*10^ (-6). The residuals were fully converged, and the solutions were stabilized, hence there was little gain in running the iterations more than 300 times.

Figure 13: Residuals graph of 2D model showing convergence at heater temperature 55.6°C

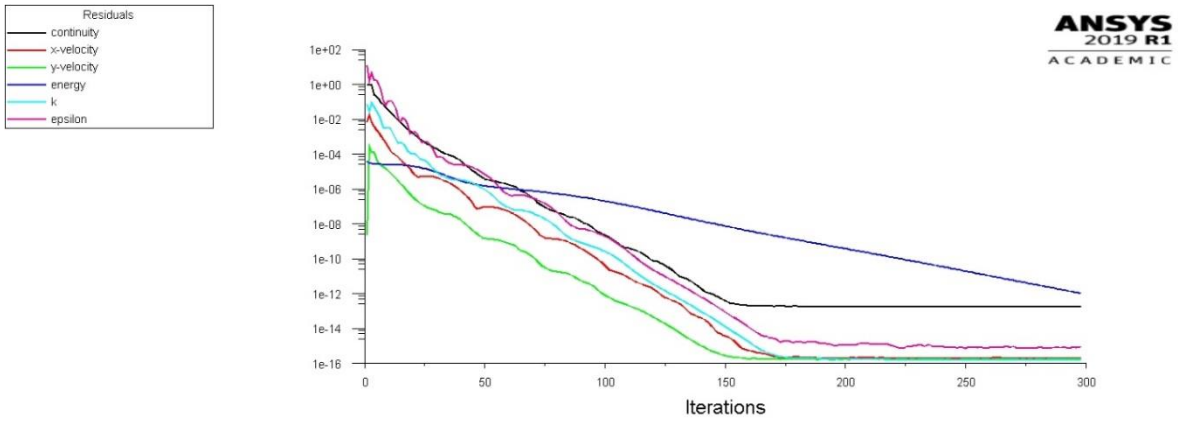

Note. Own creation.

Figure 14 depicts the radial velocity fluctuation with the position at the two ends of heat exchangers. There is no fluid movement over the walls, as illustrated in the figure due to the zero velocity across them and it demonstrates the no-slip boundary condition. The red flat line and the black line, indicates the hot fluid and the cold fluid respectively. These two lines are horizontal because of constant flow rate boundary condition at those instances. As can be observed, the cold fluid inlet and the hot fluid inlet have maximum velocities at distances of 0.008 m and 0 m, respectively. Since there is less friction near the wall, as predicted, the greatest velocity is present there.

Figure 14: Radial velocity profile of heat exchanger

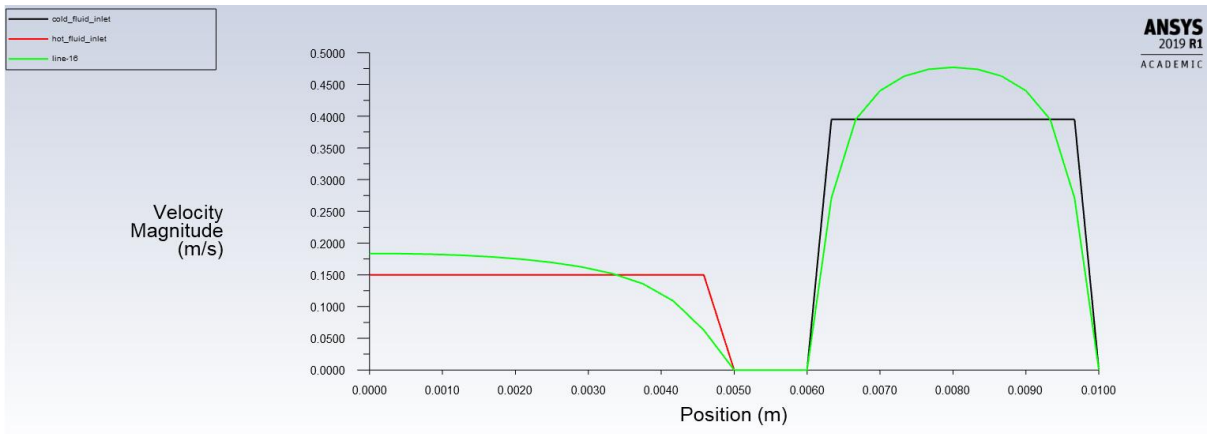

Note. Own creation.

Figure 15 depicts the radial temperature fluctuation with the position at the two ends of the heat exchanger. The temperature variation at the hot inlet to cold outlet is shown by the red line, and the temperature fluctuation at the cold inlet to hot outlet is shown by the green line. As seen in figure 15, the temperature gradient close to the wall is significantly impacted while the hot and cold flows are mostly intact or hardly altered in the middle of the flow.

Figure 15: Radial Temperature profile of heat exchanger at heater temperature 55.6°C

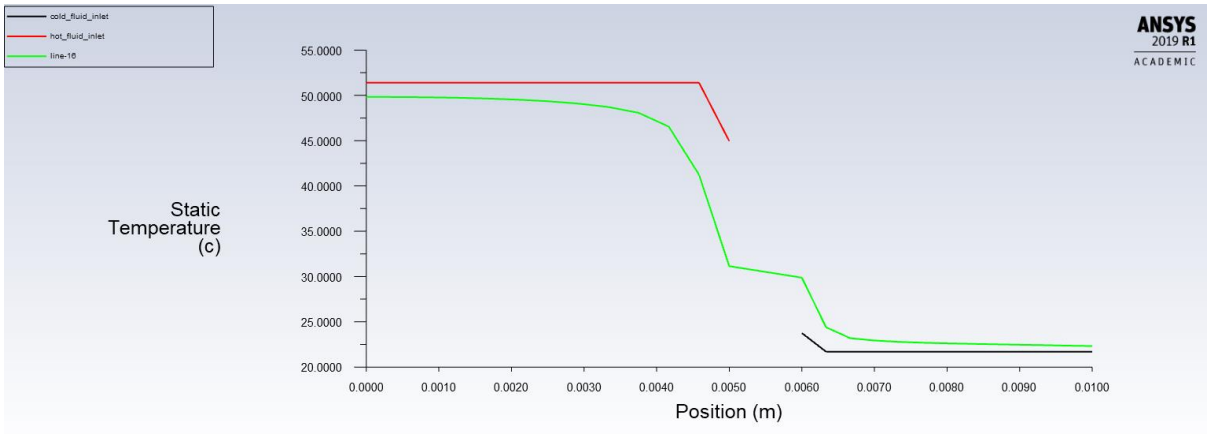

Note. Own creation.

Figure 16 depicts the 2D simulation of a pressure gradient change along the heat exchanger. The pressure gradient at the inlet pipe is maximum and the pressure is decreases as it travels axially along the pipe and has the lowest pressure at the outlet. This occurs because the increase in the velocity decreases the pressure of the flow along the pipe. The highest pressure observed at the inlet pipe was 577.1 Pa whereas the lowest at the outlet pipe was close to 0 Pa (Gage pressure).

Figure 16: Pressure change

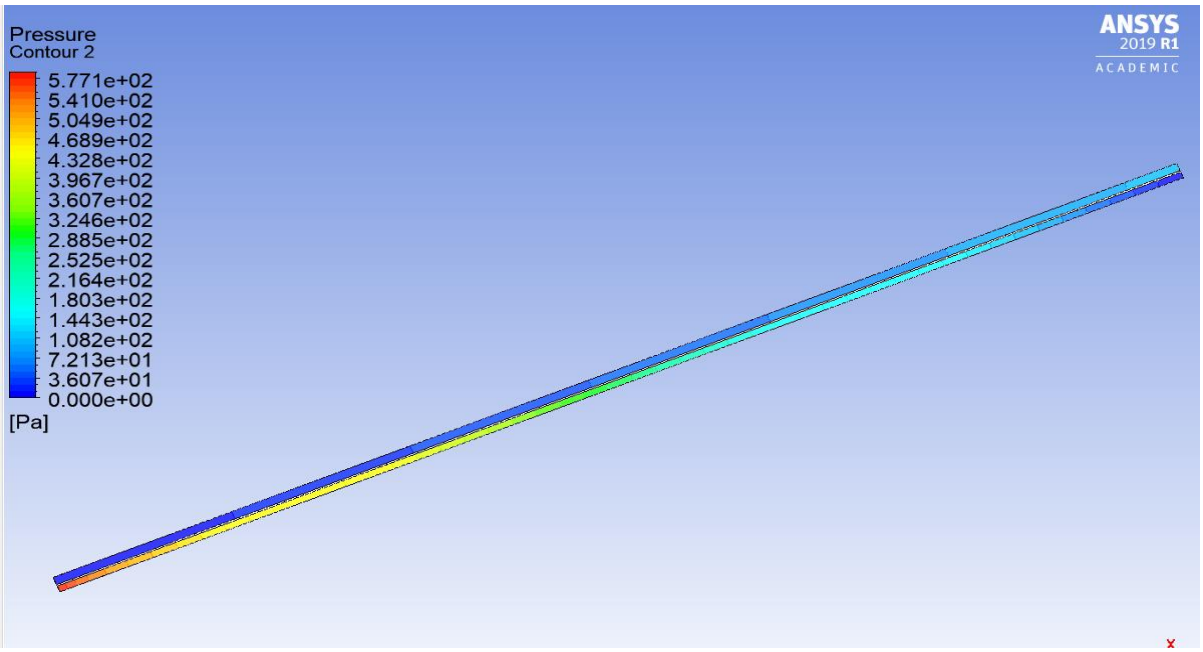

Note. Own creation.

Figure 17 depicts the 2D simulation of temperature gradient along the heat exchanger. The inner pipe temperature gradually decreases as it approaches the outlet due to the effect of cold flow from the outer pipe and the cold water on the outer pipe gains the heat due to conduction from the hot inner pipe. The inlet flow temperature in the inner pipe was set to be 323.9 K and the observed outlet temperature was close to 318.5 K. Similarly, the cold flow temperature in the outer pipe was set to be 294.9 K and observed outlet temperature was close to 298.4 K.

Figure 17: Temperature change

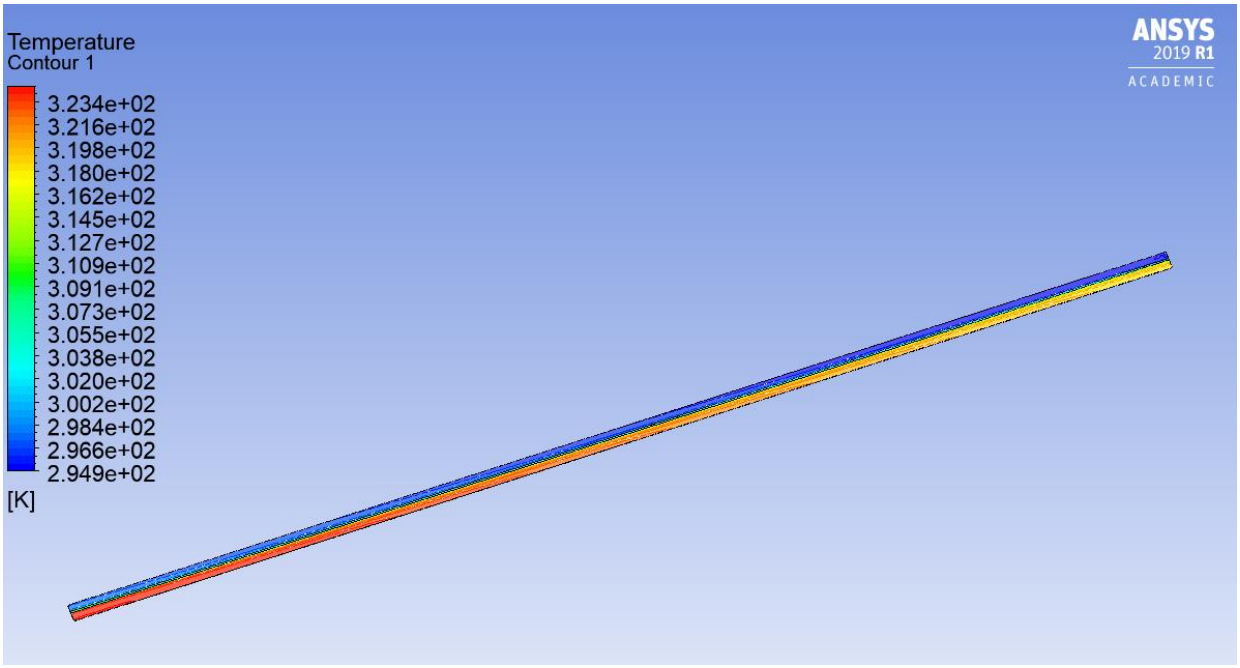

Note. Own creation.

Figure 18 depicts the change in velocity along the heat exchanger pipe. The velocity at the inlet of the inner pipe is minimum which increase as the flow travels to the outlet. It is due to the pressure decreasing along the pipe, increasing the velocity. The lowest velocity at the inner inlet was observed to be 0.395 m/s whereas the highest velocity at the outlet was 0.5158m/s.

Figure 18: Velocity change

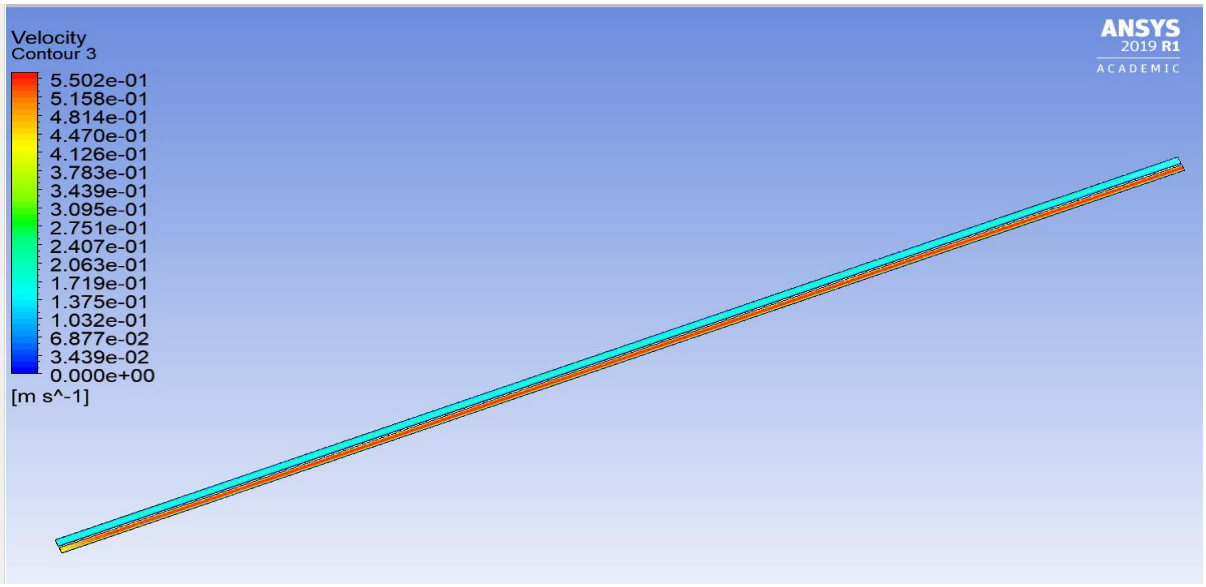

Note. Own creation.

The 2D model shows turbulence at the outlet of the pipe but it is very small as shown in figure 19. This leads to the conclusion that the 2D model isn't accurate enough to reflect turbulence across the whole system. A model with a more complex geometry (3D) is necessary to provide better results.

Figure 19: Turbulence kinetic energy change

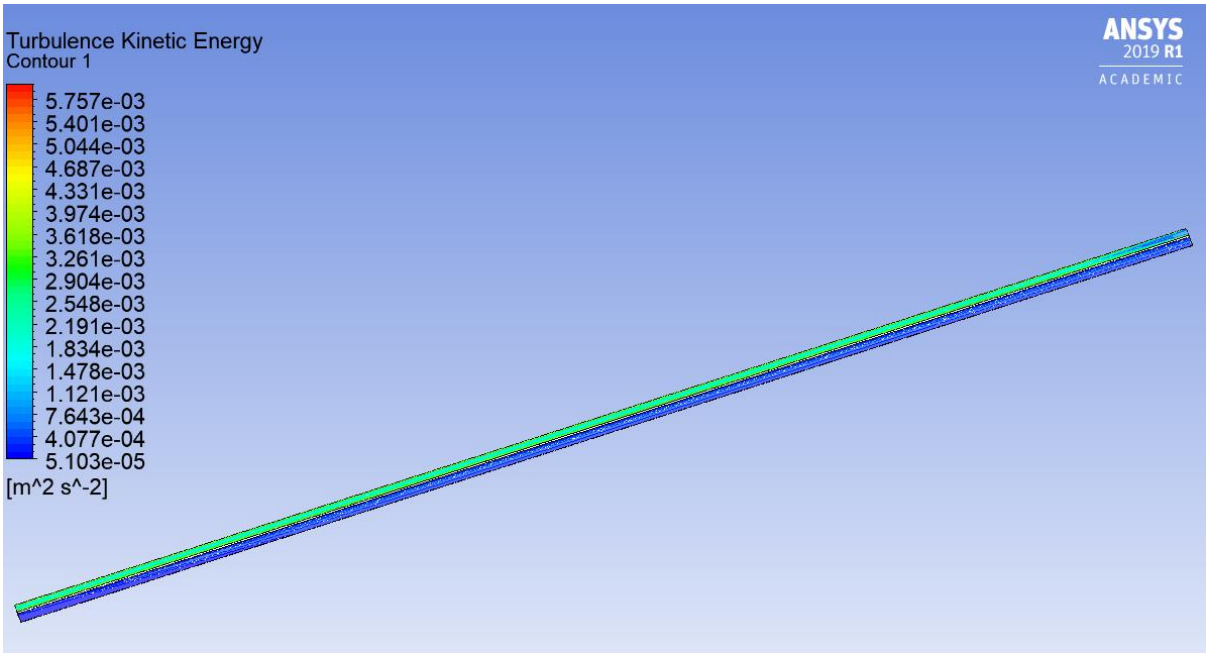

Note. Own creation.

The following tables 5 and 6 compile results from the 2D simulation recreating the experiment. The aim of this comparison is to validate the simulation results against experimental results.

Table 5: 2D simulation results for experiment 1

Hot flow, L/min	Cold flow, L/min	Th1, °C	Th2, °C	Δ Th, °C	$\overline{T_h}$, °C	Tc1, °C	Tc2, °C	Δ Tc, °C	$\overline{T_C}$, °C	$\eta_{h,\%}$	$\eta_{c,\%}$	ρ_h, kg/m^3	ρ_c, kg/m^3	C_{ph}, J/(kg K)	C_{pc}, J/(kg K)	Q_e, W	Q_a, W	C_{EB}	$\bar{\eta}$, %	LMTD, °C	U, W
0.66	1.61	51.1	44.7	6.4	47.9	20.9	22.9	1	21.9	21.19%	6.62%	989.44	997.61	4179.56	4180.18	291.13	111.90	0.38	13.91%	25.93783	561.2
0.73	1.41	51.6	45.4	6.2	48.5	20.1	22.4	1.15	21.25	19.68%	7.30%	989.14	997.47	4179.73	4180.54	311.87	112.69	0.36	13.49%	27.20342	573.2
0.73	1.19	51.4	45.8	5.6	48.6	21.6	24.1	1.25	22.85	18.79%	8.39%	989.18	997.37	5179.71	4179.76	349.09	103.35	0.30	13.59%	25.71887	678.7

Note. Own creation.

Table 6: 2D simulation results for experiment 2

Hot flow, L/min	Heater temperature, °C	Th1, °C	Th2, °C	Δ Th, °C	$\overline{T_h}$, °C	Tc1, °C	Tc2, °C	Δ Tc, °C	$\overline{T_C}$, °C	$\eta_{h,\%}$	$\eta_{c,\%}$	ρ_h, kg/m^3	ρ_c, kg/m^3	C_{ph}, J/(kg K)	C_{pc}, J/(kg K)	Q_e, W	Q_a, W	C_{EB}	$\bar{\eta}$, %	LMTD, °C	U, W
0.71	55.6	51.4	45.8	5.6	48.6	21.7	24.6	2.9	23.15	18.86%	9.76%	989.10	997.65	4179.76	4180.26	273.96	239.87	0.88	14.31%	25.43	538.7
0.8	50.2	50.0	44.2	5.8	47.1	19.4	21.5	2.1	20.45	18.95%	6.86%	989.40	997.97	4179.58	4180.95	319.79	232.20	0.73	12.91%	26.61	601.0
0.78	48.1	48.2	42.6	5.6	45.4	19.1	21.4	2.3	20.25	19.24%	7.90%	990.21	998.06	4179.15	4181.17	301.26	254.35	0.84	13.57%	25.11	599.8

Note. Own creation.

Figure 21: Experiment 1 2D simulation vs experimental results

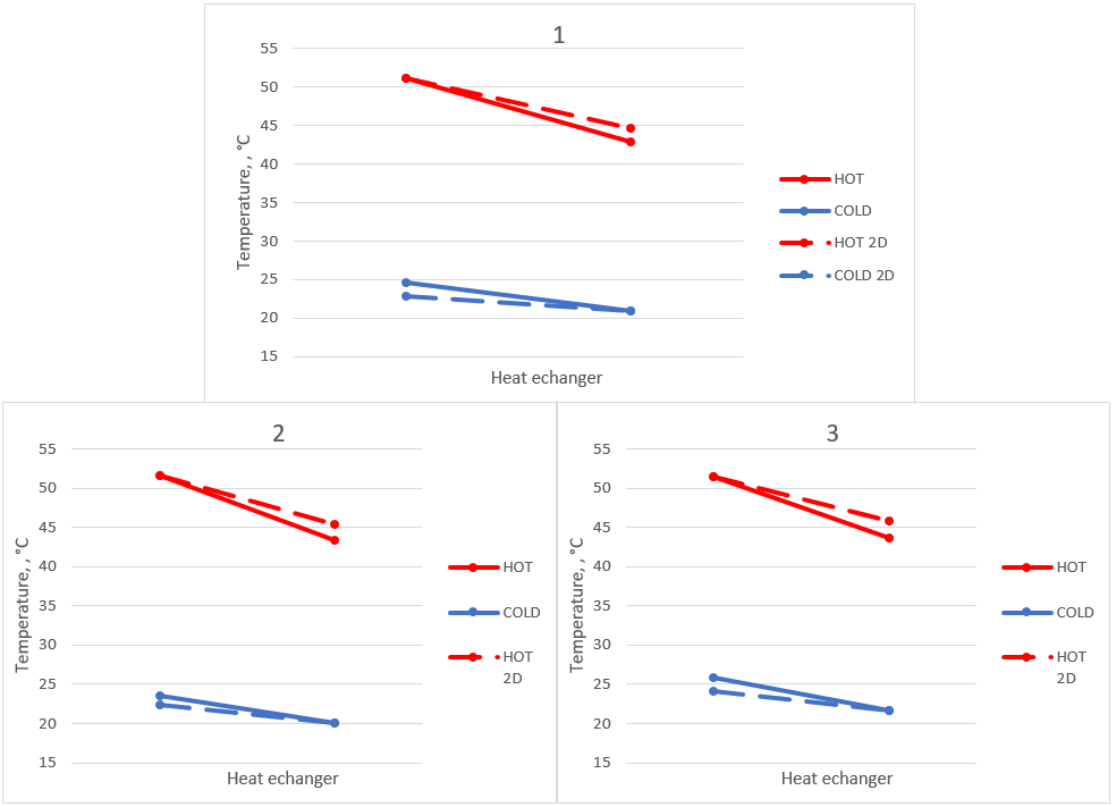

Note. Own creation.

Figure 20: Experiment 2 2D simulation vs experimental results

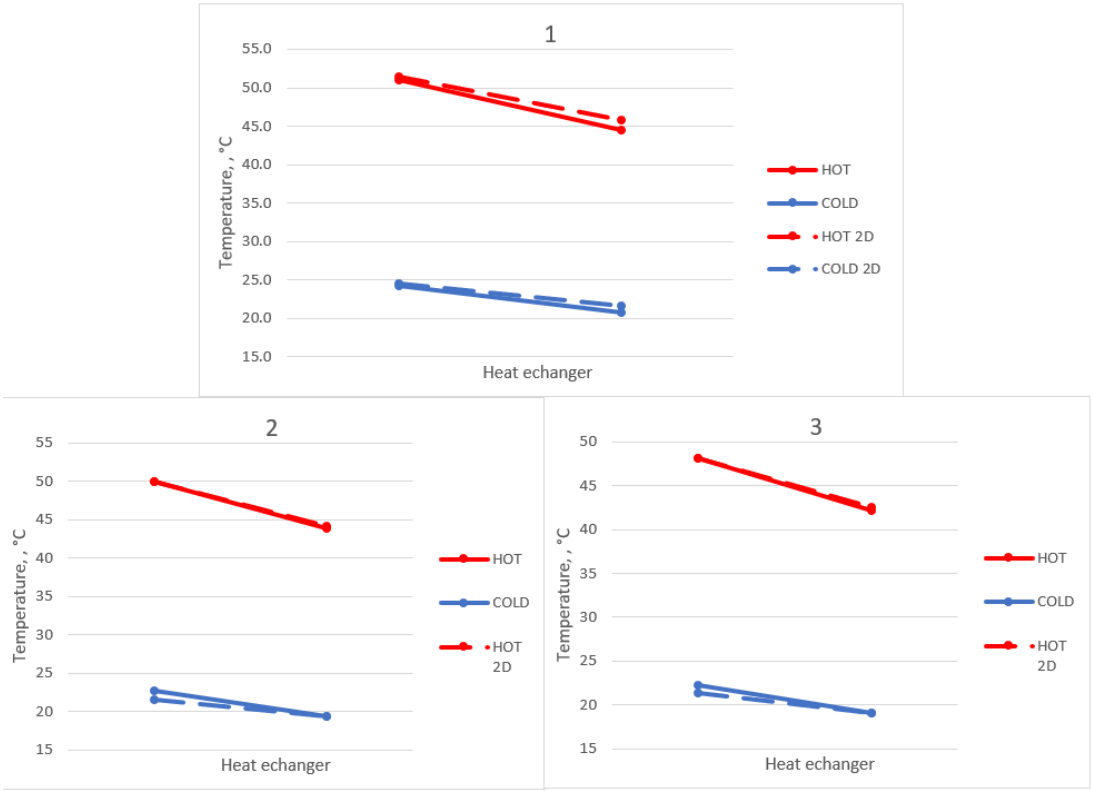

Note. Own creation.

Discussion

The results produced by the 2D simulation follow a similar trend as the experimental results, however, have a noticeable offset. This is evident in the graphs produced comparing experimental and 2D simulation results. The heat transfer coefficient for the 2D simulation in experiment 1 is significantly lower than the experimental results, however in experiment 2 this difference is not as noticeable. Likewise, the difference of hot water outlet temperatures is larger in in experiment 1. This all suggests that the true conditions of the heat exchanger were more successfully replicated in experiment 2. This can be attributed to sources of errors or possible imperfections in the created 2D model. The mean efficiency of the heat exchanger used is not great ranging from 15% to 20% for the experiment and 12% to 14% for the simulation. The fluctuation of efficiencies is greater in the experimental method, this can be attributed to less changing parameters and no unaccounted changes in the flow in the simulation. The energy balance is similarly more consistent for the simulation, for the same reasons. In the ideal condition energy balance is 1.Both the experimental and 2D results for experiment 2 achieved coefficients of energy balance closer to the ideal than experiment 1, where the energy balance for the simulation was as low as 0.3. This identifies that the parameters for the heat exchange can be greatly optimised.

Sources of errors are very important to consider when evaluating CFD models. The creation of air bubbles within the heat exchanger was observed, this decreases the efficiency and was not simulated in the CFD simulation. Even though the heat exchanger module is insulated there is still heat loss due to convection and radiation, especially in the metal joints. The flow rates and the inlet temperatures in the heat exchanger were difficult to keep constant, which complicated generating results, but does not greatly impact them. Calibration error of the sensors in the heat exchanger needs to be considered. Backflow was not accounted for and overall, the results of the 2D simulation are more consistent because errors were not considered.

The turbulence in the 2D model was almost unreadable. Diffusion processes are never completely two-dimensional, a 2D model can never adequately capture the characteristics of a turbulent system. Similarly, the k-epsilon solver was used due to the transient nature of flow which is determined calculating the Reynold's number. The K-omega solver could be another option for the simulation, and it could be used after proper research.

The element size of 3*10^ (-3) produced the same results as the element size 1.5*10^ (-3). Although the higher element size would shorten the simulation time, the simulation was conducted with simple flow, which does not increase time by a lot. The element size plays a significant role in the complex flow field. Similarly, all the residuals converged below 1*10^ (-6) which shows that the simulation has met the convergence criteria. Excellent mesh quality has an almost negligible impact on the results after a certain point as can be seen in table 2.

Conclusion

The experiment has proven the 2D simulation useful at simulating the performance of a heat exchanger, with consistent results, however the accuracy is not ideal and leaves room for improvement. The accuracy of CFD simulations depends on the quality of the model, the mesh, boundary conditions, element size, as well as the number of parameters described that have an effect on results. For these reasons to obtain the most accurate results careful consideration of every aspect affecting the problem is necessary. This leads to suggest that the more complicated the simulation is the better the results, which is why a comparison between a 2D, and a 3D model is the next step.

Bibliography

Alternative Energy Tutorials. (n.d.). *Heat Exchanger Design and Types of Heat Exchanger*. Retrieved November 9, 2022, from https://www.alternative-energy-tutorials.com/solar-hot-water/heat-exchanger-design.html

De Luca, F., Mancini, S., Miranda, S., & Pensa, C. (2016). An Extended Verification and Validation Study of CFD Simulations for Planing Hulls. *Journal of Ship Research*, *60*(2), 101–118. https://doi.org/10.5957/JOSR.60.2.160010

Edge., E. (2019, nd nd). *Parallel and Counter Flow Designs.* Retrieved from Enginers Edge.: https://www.engineersedge.com/heat_transfer/parallel_counter_flow_designs.htm

Electrical Workbook. (2022). *What is Multipass Heat Exchanger? Construction, Working, Diagram & Applications - ElectricalWorkbook*. https://electricalworkbook.com/multipass-heat-exchanger/

Engineers Edge. (2022). *Parallel and Counter Flow Designs Heat Exchangers*. https://www.engineersedge.com/heat_transfer/parallel_counter_flow_designs.htm

Linquip. (2021). *Cross Flow Heat Exchangers: All Practical Guides You Should Know*. https://www.linquip.com/blog/cross-flow-heat-exchangers/

Qubeissi, M. (2022). *CW1 brief*.

https://coventry.aula.education/?#/dashboard/b1d9645d-de7a-4c7d-9ad3-2d0c17295179/journey/materials/de79dab3-9e52-4704-997a-85196ddf2b2a

Team, L. (2021, 15 March). *What are Counter Flow Heat Exchangers and its Working Principles?* Retrieved from Linquip Technews: https://www.linquip.com/blog/counter-flow-heat-exchangers/#:~:text=What%20is%20a%20Counter%20Flow%20Heat%20Exchanger%3F&text=Counter%20Flow%20Heat%20Exchangers%20are,can%20be%20counter%20flow%20exchanger.

Tips., F. (2021, May 07). *How to Verify Mesh Quality in ANSYS Workbench*. Retrieved from FEA TIPS: https://featips.com/2021/05/07/how-to-verify-mesh-quality-in-ansys-workbench/

Appendix

Appendix A. Residuals graph of 2D model showing convergence at heater temperature 48.1°C

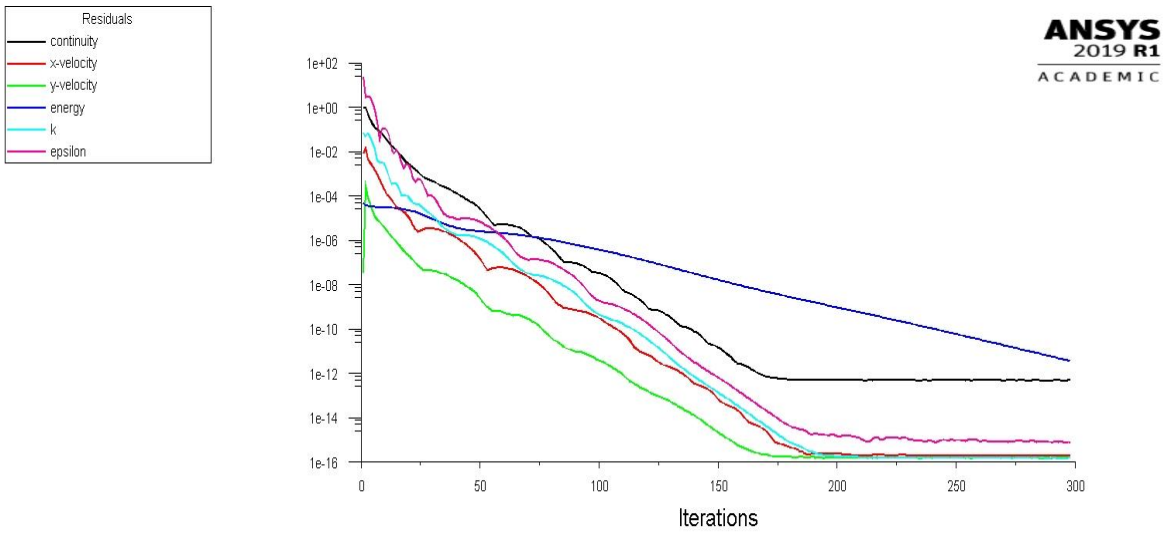

Appendix B. Residuals graph of 2D model showing convergence at heater temperature 50.2°C

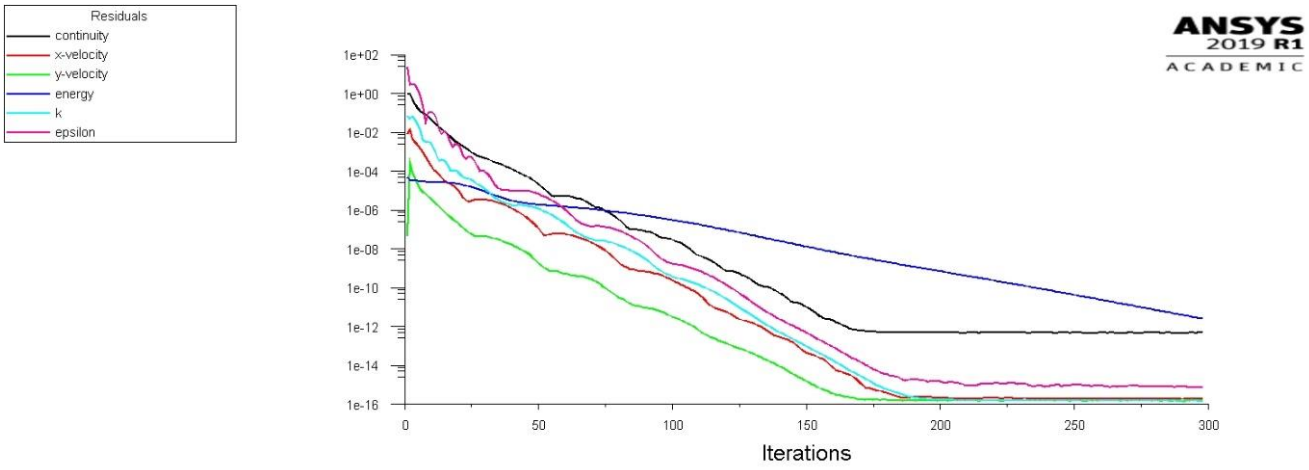

Appendix C. Residuals graph of 2D model showing convergence at flow rate of 1.2 L/m.

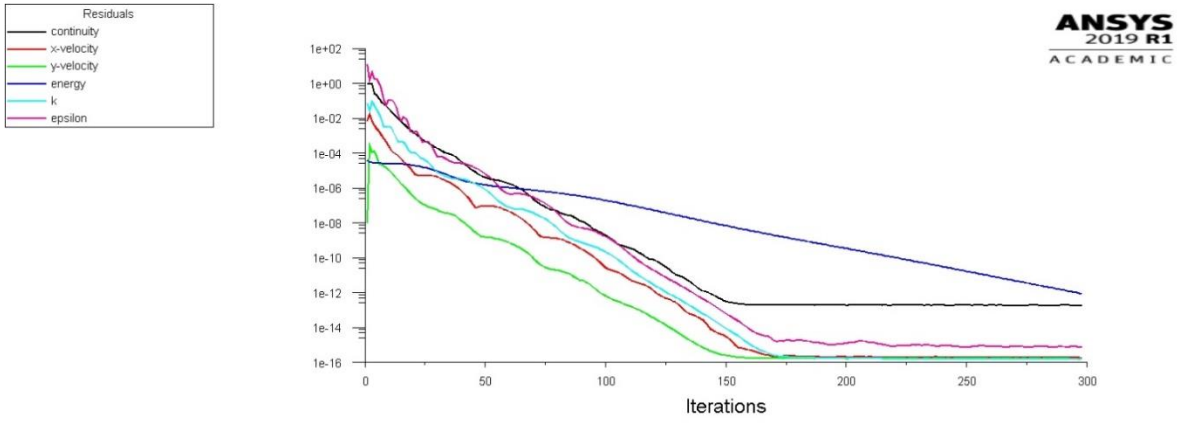

Appendix D. Residuals graph of 2D model showing convergence at flow rate of 1.4 L/m.

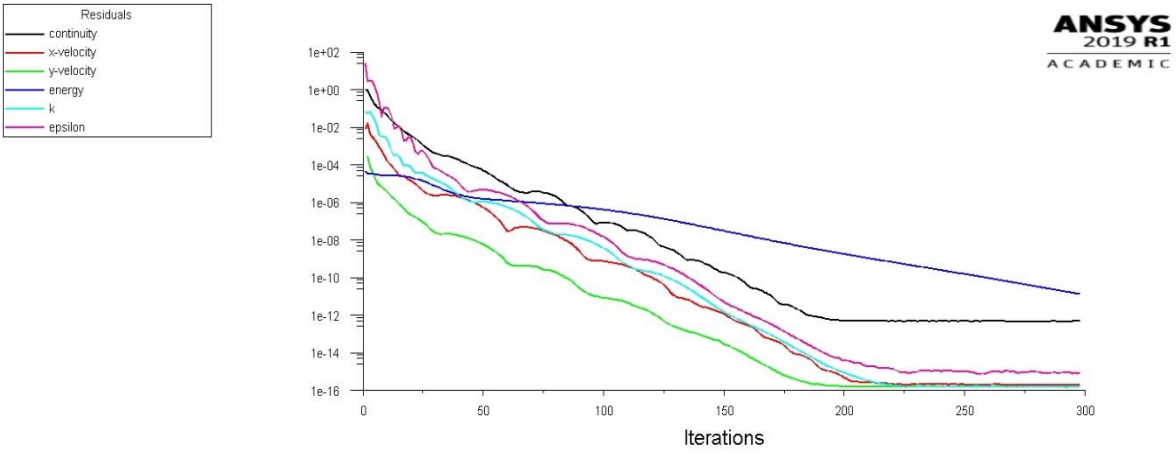

Appendix C. Residuals graph of 2D model showing convergence at flow rate of 1.6 L/m.